

## Small-cluster analogs of CO adsorption on Cu/Ru(0001): Total-energy and carbon-metal stretch frequency calculations

Pei-Lin Cao,\* D. E. Ellis, A. J. Freeman, and Qing-Qi Zheng†  
*Physics Department, Northwestern University, Evanston, Illinois 60201*

S. D. Bader

*Materials Science and Technology Division, Argonne National Laboratory, Argonne, Illinois 60439*

(Received 16 April 1984)

Total energies as a function of carbon-metal-layer separation and carbon-metal perpendicular stretch frequencies are calculated for small clusters configured to be analogs for the chemisorption system CO on Cu/Ru(0001). The clusters (with 7–10 metal atoms) include analogs of CO/Cu(111) and CO/Ru(0001) with on-top and threefold binding sites. The latter are more stable in both cases. Mixed-metal clusters are also studied (i) with CO bound to Cu in proximity to Ru and (ii) with CO bound to Ru in proximity to Cu. The former, case (i), show enhanced CO binding with respect to CO on pure Cu, and the latter, case (ii), show weakened CO binding with respect to CO on pure Ru. Possible precursor intermediate states are described for commensurate and incommensurate epitaxy. Bonding to Ru sublayers through a Cu adlayer is also described. The results are discussed in conjunction with previous experimental findings, and anticipate future experimental vibrational characterizations.

### INTRODUCTION

The properties modifications that occur in epitaxial metal films have been the subject of much recent interest. Three types of films may be distinguished: (i) monolayer, (ii) multilayer, and (iii) repetitive multilayer structures. At the monolayer stage<sup>1,2</sup> interest arises from the ability to influence chemisorption and catalytic properties, as well as magnetic-moment formation. A prime focus of multilayer film research is to create, by epitaxy, new structures that do not otherwise exist in nature.<sup>3</sup> For repetitive multilayers it is possible to make artificial superlattices, and hence introduce long periodicities that nature does not otherwise provide.<sup>4</sup> For all of these systems electron spectroscopic characterizations during the growth period can yield valuable information concerning the quality of the interfacial region, as well as its electronic properties.

In the present work, we are concerned with monolayer structures for the system Cu-covered Ru(0001). Interest in this system stems from the general observation that coating a group-VIII transition metal with a group-IIb metal improves various desirable catalytic properties, such as selectivity and activity.<sup>5</sup> Ru is a prime Fischer-Tropsch catalyst, as well as a dehydrogenation and hydrogenation catalyst. Within the surface-science community there has been recent interest in understanding the electronic structure and elementary chemisorption processes that occur on related epitaxial metal systems. Some examples include recent Cu/Pt (Ref. 6) and Au/Pt (Ref. 7) experiments and Ag/Rh (Ref. 8) and Au/Pt (Ref. 9) band-structure investigations.

For the Cu/Ru system there have been extensive experimental<sup>1,2,10–14</sup> and theoretical<sup>1,15</sup> studies. We summarize now the highlights of those investigations that have bearing on the present work. Cu was found to grow epitaxial-

ly<sup>10</sup> on Ru(0001) with the Cu(111) orientation and [101]||[1010]. The growth depends on substrate temperature and can be initially described by a layer-by-layer mechanism. The epitaxy is believed to be incommensurate, however, with both Cu(111) and Ru(0001) retaining their bulk in-plane lattice spacings. This leads to a 5% mismatch in lattice constants. Photoemission results<sup>2</sup> indicated for monolayer stage films that the Cu *d* band narrowed, as expected, but also shifted to higher binding energy by ~0.6 eV compared to bulk Cu. Similar shifts were then observed in the Cu/Ru versus pure Cu self-consistent film calculations by Ma *et al.*,<sup>15</sup> who used their recently-developed linearized muffin-tin orbital approach. They attributed their observations to a charge transfer from Ru to Cu, as had been inferred experimentally as well. To lend credence to their result, they found no such charge-transfer effect when they similarly treated the Cu/Ni system, in accord with expectation. Recently corrected work-function measurements were also interpreted to indicate "a net charge transfer from the Ru to the Cu on top."<sup>13</sup>

Experimentally, the CO molecule was introduced as a well-understood probe molecule of the surface. Differences were found in CO adsorption characteristics of both the Ru and Cu binding sites relative to those found on the pure metals. CO adhered to Ru more weakly when Cu was in proximity, and more strongly to Cu when Ru was in proximity. These conclusions were drawn from thermal desorption studies using both conventional<sup>2,12</sup> and novel photoemission detection<sup>1</sup> techniques. Photoemission at 40.8-eV photon energy of the CO-saturated surface served as a valuable characterization technique since the CO-derived emissions from the perturbed Ru and Cu sites in the epitaxial film were sharp and occurred at separated binding energies.<sup>1</sup> The CO binding-energy changes observed experimentally can be understood qualitatively

within the context of Ru-to-Cu charge transfer, as supported by the calculations of Ma *et al.*<sup>15</sup> It is well known that the strength of the metal-CO bond is controlled by "back bonding" or metal charge donation to the antibonding  $2\pi^*$ -derived CO orbitals.<sup>16</sup> Within this framework CO bound to Ru in proximity to Cu can be viewed as a competitive coadsorption system. Both Cu and CO compete for charge from Ru; the relatively strong Ru-Cu bonding leaves the Ru-CO bond weakened relative to that of pure Ru-CO. For CO bound to Cu in proximity to Ru, the charge transfer from Ru to Cu enhances the charge transfer from Cu to CO, and hence the Cu-CO bond strengthens relative to that of pure Cu-CO.

To make contact with catalytic applications the weakening of the Ru-adsorbate bond when Cu is in proximity seems to be the more important effect as opposed to the corresponding Cu-adsorbate bond strengthening that occurs. This is because for the latter desorption occurs below room temperature, while for the former desorption occurs above, i.e., at catalytic-process temperatures. The approximate binding energy for Ru-CO is 29 kcal/mole,<sup>17</sup> and for Cu-CO is only 12 kcal/mole.<sup>18</sup> The former is reduced  $\sim 25\%$  in the epitaxial configuration,<sup>1</sup> while the latter is enhanced  $\sim 25\%$ .<sup>2</sup> Thus, the transition metal remains the catalytic species, but reactions that require strong metal-adsorbate interactions can be selectively shut off. For instance, in the hydrogenolysis-dehydrogenation competition<sup>5</sup> the hydrogenolysis process becomes less important because it requires severing C-C bonds, which, in turn, requires strong C-metal (catalyst) bond strengths. Of course this is not the sole effect that influences catalytic selectivity, but it is widely regarded as one of the key effects. Also, in the above, the CO results were generalized to other adsorbates. While this cannot be done indiscriminately, adsorbates with similar electron donor-acceptor (Lewis acid-base) characteristics are expected to behave qualitatively similarly.<sup>19</sup>

Thus, it is of interest to pursue further our understanding of the Cu/Ru prototype surface and the insights derived from the CO probe-molecule experiments. To this

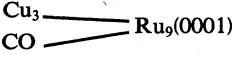
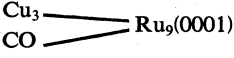
end in the present work, small-cluster analogs of the species of interest were constructed and the total energies were calculated as a function of the height  $h$  of the CO carbon atom above the metal surface. Preliminary results<sup>1</sup> have been reported previously, but the present results are improved in that the geometrical stacking errors of the previous calculations are corrected, more complete basis sets were used and tested, more geometric configurations were modeled, and more values of  $h$  were used, especially near minima and local minima in the total energy. Most importantly, the present results have been used to estimate the carbon-metal stretch frequency associated with each cluster simulation. These results suggest that experimental vibrational analysis should serve as a valuable probe to test the veracity of the computations, and thus, the insights provided. In particular, the calculations indicate that threefold binding sites are more stable than on-top sites for both Cu(111) and Ru(0001) clusters, and that for CO bound to Ru, in proximity to Cu, a possible precursor intermediate to desorption can be described.

## II. METHODS

### A. Description of clusters

Table I contains a description of the clusters studied. They are grouped into four types, labeled I through IV, in analogy with the four types of CO-surface interactions identified experimentally.<sup>1</sup> These are, respectively, CO-pure copper interactions, CO-copper perturbed by Ru, CO-ruthenium perturbed by Cu, and CO-pure ruthenium interactions. For each type of interaction there were two cluster systems studied with  $C_{3v}$  point-group symmetry. A bird's-eye view of each cluster is given in Figs. 1-3, along with the binding-energy curves (except for the pure Cu clusters which appear in Ref. 1). For the pure-metal types I and IV the cluster labeled *a* has the CO located at a threefold-symmetric metal binding site. The corresponding *b* cluster is for a onefold, or on-top, geometry. Of course, the bonding is with the carbon end of the molecule pointed toward the surface; the molecule axis is taken

TABLE I. Description of clusters.

Type	Cluster	CO binding-site symmetry	Comments
Ia	CO-Cu <sub>7</sub> (111)	threefold	
Ib	CO-Cu <sub>10</sub> (111)	on top	
IIa	CO-Cu <sub>3</sub> -Ru <sub>9</sub> (0001)	threefold	perturbed Cu-CO
IIb	CO-Cu <sub>3</sub> -Ru <sub>10</sub> (0001)	threefold	
IIIa		threefold	} commensurate Cu-Ru } perturbed Ru-CO } Cu at 2 NN position } 5% contracted Cu
IIIb		threefold	
IVa	CO-Ru <sub>9</sub> (0001)	threefold	
IVb	CO-Ru <sub>10</sub> (0001)	on top	

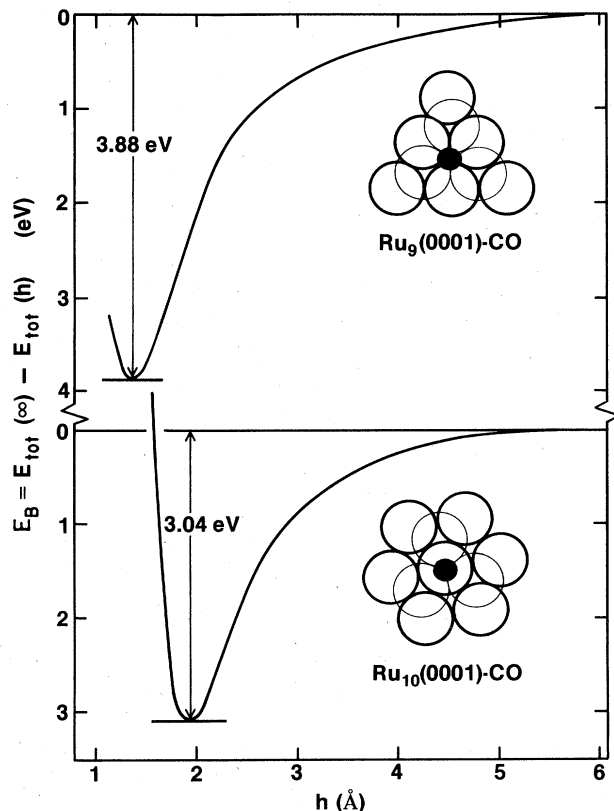


FIG. 1. Binding energies as a function of the height of the CO carbon atom above the Ru surface layer for the indicated clusters (type IV *a* and IV *b* of Tables I and II). Insets describe threefold (top panel) and on-top (bottom panel) CO binding site symmetry; the thick open circles depict top-layer Ru atoms, thin open circles depict second-layer Ru atoms, and the solid circle indicates the CO position.

perpendicular to the surface. For the mixed-metal cluster types II and III, threefold binding sites were chosen throughout. The difference between II *a* and II *b* is that the ruthenium layer underlying the copper layer is also threefold coordinated with the CO for *a*, but has an on-top-type geometry with respect to the CO for *b*. This corresponds in a manner to the two kinds of threefold sites found on the basal plane. For cluster III *a* the Cu atoms are located at second-nearest-neighbor sites, so that the CO clearly has room to bond directly to the Ru through the Cu adlayer. For cluster III *b*, the Cu atoms are symmetrically moved within the plane toward the CO molecule by an arbitrary 5%. This was done to explore the effect of increasing the Cu interactions with CO. Also, it is known experimentally that the Cu atoms can be out of registry with the Ru(0001).

### B. Description of the calculations

The one-electron Hamiltonian in the local-density  $\chi\alpha$  model has been used in these studies. In Hartree atomic units, it is given by

$$H(\vec{r}) = -\frac{1}{2}\nabla^2 + V_C(\vec{r}) + V_x(\vec{r}), \quad (1)$$

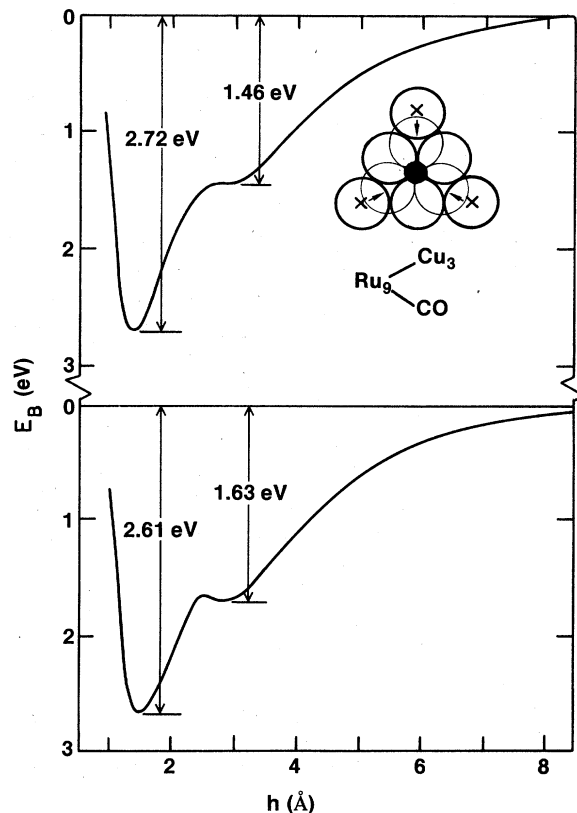


FIG. 2. Binding energies vs  $h$  for cluster types III *a* (top) and III *b* (bottom). The inset describes the  $\text{Ru}_9\text{-CO}$  geometry as in the top panel of Fig. 1, except that three Cu atoms, denoted by the  $\times$  symbols, are coadsorbed on the Ru surface at second-nearest-neighbor positions to the CO. The arrows denote the direction of the 5% contraction of the Cu atoms appropriate to the bottom panel results.

where  $V_C$  is the Coulomb potential

$$V_C(\vec{r}) = \sum_j \frac{-Z_j}{|\vec{r} - \vec{R}_j|} + \int d^3\vec{r}' \frac{\rho(\vec{r}')}{|\vec{r} - \vec{r}'|}, \quad (2)$$

and  $V_x$  is a statistical exchange potential of the form<sup>34</sup>

$$V_x(\vec{r}) = -3\alpha \left[ \frac{3}{8\pi} \rho(\vec{r}) \right]^{1/3}. \quad (3)$$

In (2) and (3),  $\rho(\vec{r})$  is the electron density at position  $\vec{r}$ , and  $\alpha$  is an exchange-correlation scaling parameter which is normally chosen as  $\frac{2}{3} \leq \alpha \leq 1$ . Here it is chosen to be 0.7 for all calculations.<sup>20</sup>

The molecular wave functions are approximated by a linear combination of symmetry orbitals  $\phi_i(\vec{r})$  as

$$\psi_n(\vec{r}) = \sum_i \phi_i(\vec{r}) C_{in}, \quad (4)$$

where the symmetry orbitals are taken to be linear combinations of numerical atomic functions centered on the nuclei. The solution of the secular matrix equation

$$\underline{HC} = \underline{ESC} \quad (5)$$

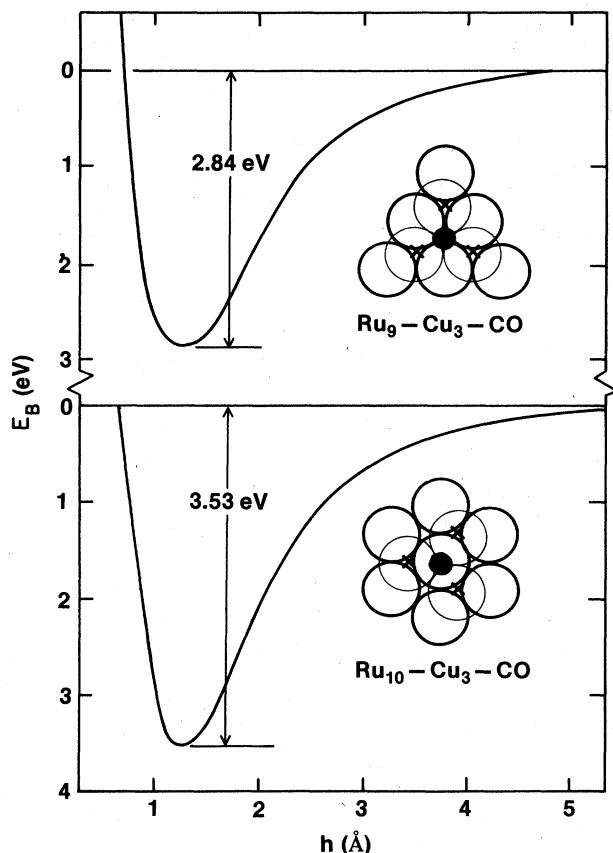


FIG. 3. Binding energies vs  $h$  for CO adsorbed to a Cu layer on the indicated Ru clusters. The insets are top views of the clusters with the same symbol designations as in Figs. 1 and 2. The top (bottom) panel results are for clusters IIa (IIb) of Tables I and II.

determines the coefficients  $C_{in}$  where  $\underline{H}$  and  $\underline{S}$  represent the Hamiltonian and the overlap matrices, respectively. The discrete variational method (DVM) is used to calculate the matrices  $\underline{H}$  and  $\underline{S}$  by a numerical integration procedure with a weighted sum over a set of (relatively few) sample points.<sup>21</sup>

The molecular wave functions and eigenvalues were determined using the self-consistent charge (SCC) approximation to the potential.<sup>22,23</sup> From Mulliken gross orbital populations<sup>24</sup> for the symmetrized basis functions, the cluster charge density was decomposed approximately as

$$\begin{aligned} \rho_{\text{cluster}} &= \sum_i f_i |\psi_i(\vec{r})|^2 \\ &\simeq \sum_{\nu, n, l} f_{n1}^{\nu} |R_{n1}(r_{\nu})|^2 = \rho_{\text{SCC}}, \end{aligned} \quad (6)$$

where  $f_i$  is the occupation number for the  $i$ th eigenvector which is determined by Fermi-Dirac statistics and  $f_{n1}^{\nu}$  is the population for atom  $\nu$  of the  $nl$  atomic orbital. Self-consistency is obtained when the input and output atomic-orbital populations are equal.

The basis functions were obtained from numerical solutions of the free-atom problem. In the present procedure

the Cu  $1s \cdots 3p$  and the Ru  $1s \cdots 4p$  core orbitals have not been varied; that is, we have used a "frozen-core" approximation. For the valence electrons the Cu  $3d$ ,  $4s$ , and  $4p$  and Ru  $4d$ ,  $5s$ , and  $5p$  orbitals are included in the variational procedure.

The self-consistent single-particle energies,  $E_i$ , can be used to generate densities-of-states diagrams, and these have been used extensively in interpretations of photoelectron spectra for chemisorbed species.<sup>23</sup> In general, one observes in the present case peaks associated with the CO  $\pi$ - and  $\sigma$ -symmetry orbitals broadened by interaction with the substrate and superimposed upon substrate emission. In addition, one finds "antibonding states" or resonances above the Fermi energy which can be correlated to electron energy loss and other spectroscopies that probe empty states.

The position of calculated photoemission peaks depends upon surface geometry, and thus by matching calculated peaks with experimental data one obtains a prediction of the local molecular configuration of the chemisorbed species. This procedure is rather limited, however, due to the intrinsic line broadening and superposition of emissions in experiment, and due to final-state relaxation effects and other computational limitations. Of course, no information about relative stability or absolute molecular binding energies is obtained from the single-particle spectra.

A technically difficult, but logically straightforward approach is to calculate the total energy, given in the simplest local-density approximation [see Eqs. (1)–(3)] as

$$E_{\text{tot}}(\rho) = \sum_i f_i E_i - \frac{1}{2} W_{\text{Coul}} - \frac{1}{4} W_x. \quad (7)$$

Here  $W_{\text{Coul}}$  and  $W_x$  represent Coulomb and exchange energies which are "double-counted" in the single-particle sum.<sup>20</sup> In practice, we calculate binding energies in the form

$$-E_B(\rho) \approx E_{\text{tot}}(\tilde{\rho}) - E_{\text{tot}}(\rho_{\text{ref}}), \quad (8)$$

where  $\tilde{\rho}$  is some analytic approximation to the true density  $\rho$ , and  $\rho_{\text{ref}}$  is the density of the reference state—e.g., CO removed to a large distance from the substrate. By this means we are able to calculate the binding energy (BE) to a precision of 0.1 eV or better. In the remainder of this paper we will concentrate on aspects of the binding-energy results.

### III. RESULTS AND DISCUSSION

Table II contains a summary of the results of the total-energy calculations as a function of the carbon-metal layer separation  $h$ . Included in Table II are the equilibrium separations  $h_{\text{eq}}$  and the corresponding binding energies relative to  $h = \infty$ . Also included are the force constants  $\phi''$  and carbon-metal-layer perpendicular stretch frequencies  $\omega$ . The quantity  $\phi''$  was obtained in each case from a harmonic-model analysis of the bottom region of the potential well. Closely spaced total-energy calculations were made near  $h_{\text{eq}}$ . Parabolic equations were least-squares fitted in a similar manner for each cluster, and the spring constant was extracted. To convert  $\phi''$  into the stretch

TABLE II. Summary of results.

Type	BE (eV)	$h_{eq}$ (Å) (C-metal)	$\phi''$ $\left[ \frac{eV}{\text{Å}^2} \right]$	$\omega$ (meV)
Ia	1.7	1.36	9.95	52
Ib	0.78	1.93	7.63	32
IIa	2.84	1.25 <sup>a</sup>	2.44	24
IIb	3.53	1.26 <sup>a</sup>	7.25	41
IIIa	2.72 (1.46) <sup>b</sup>	1.48 (3.02) <sup>b</sup>	5.24	37
IIIb	2.61 (1.63) <sup>b</sup>	1.48 (2.80) <sup>b</sup>	5.32	38
IVa	3.88	1.37	11.76	53
IVb	3.10	1.94	10.59	45

<sup>a</sup>The Cu-Ru separation was set fixed at 2.09 Å.

<sup>b</sup>Properties of subsidiary minimum also shown.

frequency  $\omega$ , first-order finite-mass corrections were made as described in Ref. 25. This takes into account the fact that the spring is not anchored to an infinite mass on one end, as in the simplest model. For the purposes of this correction, the mass of the adsorbate was taken as the mass of carbon plus oxygen. This is justified since the carbon and oxygen should move rigidly in phase for this mode of vibration, especially at the Brillouin-zone center, where most comparisons are made to high-resolution electron-energy-loss spectroscopy experiments.

#### A. Survey of qualitative expectations

An examination of the binding-energy values contained in Table II shows that a number of qualitative expectations are met. For instance, CO is more strongly bound to the type-IV pure Ru clusters than to the type-I pure Cu clusters. The type-III Cu-perturbed Ru-CO clusters show *weakened* CO binding energies compared to the type-IV pure Ru-CO clusters. Also, the type-II Ru-perturbed Cu-CO clusters show *enhanced* CO binding energies compared to the type-I pure Cu-CO clusters. While these observations are consistent with those outlined in the Introduction, there is also much new information, as described below.

#### B. Pure-metal clusters

From Table II we see that for the type-I and -IV pure-metal clusters threefold binding sites are more stable than are onefold. It had been conjectured that the opposite would be true, at least for CO bound to single-crystal Ru(0001). This was based on a widely-used correlation found experimentally for carbonyl clusters,<sup>26</sup> between the strength of the C-O stretch frequency  $\omega_{CO}$  and the binding-site symmetry. For an on-top geometry the value of  $\omega_{CO}$  tends to be  $\geq 2000$   $\text{cm}^{-1}$ , while for a threefold geometry  $\omega_{CO}$  is  $\leq 1900$   $\text{cm}^{-1}$ . Thomas and Weinberg<sup>27</sup> measured  $\omega_{CO}$  for CO/Ru(0001) and found a value of 1990  $\text{cm}^{-1}$  which suggested to them on-top bonding. However, they also report a carbon-metal stretch frequen-

cy of 55 meV (445  $\text{cm}^{-1}$ ). This compares quite favorably with the calculated value of 53 meV for the more stable threefold binding-site symmetry of cluster IVa in Table II. The corresponding value for the on-top-geometry cluster IVb is only 45 meV. What is of interest here is that even for the CO—pure-metal systems important questions still exist concerning geometry.<sup>28</sup> Also, the interplay of computational and experimental investigations helps to focus attention on such questions. For CO/Cu(100) the carbonyl analogy works. It predicts on-top binding based on the measured  $\omega_{CO}$  (Ref. 29) value of 2090  $\text{cm}^{-1}$ . For this system on-top binding has been demonstrated, based on comparisons between calculated and measured vibrational features that appear within the substrate phonon region.<sup>30</sup> However, even such sophisticated comparisons can be misleading, as the O/Ni(100) controversy has demonstrated.<sup>31,32</sup> State-of-the-art solutions to such problems now involve fitting the phonon dispersion curves along high-symmetry directions of the Brillouin zone,<sup>31</sup> as opposed to being limited to  $\Gamma$ -point comparisons between experiment and calculation.

#### C. Mixed-metal clusters

The type-IIIa and IIIb clusters have very similar properties. It is logical to discuss them before the type-II clusters, as will become clear below. In cluster IIIa, the carbon atom of the CO molecule at equilibrium bonds to the threefold Ru site through the opening in the Cu adlayer. Comparison to the pure-metal situation of cluster IVa shows that the proximity of the Cu atoms at second-nearest-neighbor positions in cluster IIIa weakens the Ru-CO bonding. This is reflected in the drop in CO binding energy from 3.88 to 2.72 eV, and the increase in  $h_{eq}$  from 1.37 to 1.48 Å. The total-energy curve (see Fig. 2) shows a subsidiary minimum at 3.02 Å of 1.46-eV well depth. This corresponds to the CO lifting off the Ru layer but being weakly attracted to the Cu layer. At the subsidiary minimum the carbon is 0.93 Å (=3.02–2.09 Å) above the Cu layer. This close approach compared to

the value 1.36 Å for the pure Cu-CO cluster Ia is permitted since the nearest-neighbor Cu atoms are missing and the bonding is to next-nearest neighbors. We pointed out previously<sup>1</sup> that this metastably-bound CO provides an interesting possible precursor intermediate state to desorption, and that descriptions of such states are usually elusive.

It is known experimentally<sup>10</sup> that the Cu layer adatoms can occupy positions out of registry with those of the Ru substrate. In the mixed-metal cluster IIIa discussed above, the Cu atoms were positioned *in* registry with the Ru. In cluster IIIb, the three Cu atoms are removed from their commensurate second-nearest-neighbor positions and arbitrarily contracted in the plane 5% symmetrically toward the CO binding site. Comparison of the results for cluster IIIa and IIIb shows that this movement tightens the metastable Cu-CO bond. The well depth increases from 1.46 to 1.63 eV and the  $h_{eq}$  value decreases from 3.02 to 2.80 Å. There is also a modest decrease in the Ru-CO well depth from 2.72 to 2.61 eV. (Note as well that the calculated  $\omega$  values for the type-III clusters are highly insensitive to this Cu-layer contraction.) The important trend to remember is that an increased Cu-CO bond strength is accompanied by a decreased Ru-CO bond strength. This trend will be useful in understanding the bonding of cluster type II which we now discuss.

For the type-II clusters the CO is above the Cu adlayer. Again, a threefold binding symmetry was chosen, since the threefold site was more stable than the on-top site in the pure Cu-CO calculation of cluster Ia. As was pointed out earlier, the qualitative expectation is met that the Cu-CO bond is more stable when the Cu is in proximity to Ru than for pure Cu. The problem is that quantitatively the binding energies are extremely high (2.84 and 3.53 eV) compared to that for pure Cu (1.7 eV) or even to the type-III mixed-metal clusters (2.72 and 2.61 eV). We think that the way to intuitively understand the numerics is to visualize the creation of the type-II cluster from a continuation of the contraction that transformed cluster IIIa into IIIb. As the Cu atoms are brought into nearest-neighbor positions, the subsidiary minimum in the total-energy curve will deepen relative to the primary minimum and will shift in position toward it. Eventually the two minima will merge, corresponding to CO bound to Cu and Ru sites. The binding energy, being a sum of the two component contributions, can significantly exceed that of CO bound only to Cu. In this regard it is interesting to note that in cluster IIb, which has the very large 3.53 eV binding energy, there is a single Ru atom coordinated below the Cu threefold site. To estimate the strength of the binding to this Ru atom we refer to the total-energy curve for cluster IVb at the Ru-CO separation that corresponds to equilibrium for cluster IIb. The contribution is only  $\sim 0.6$  eV. If we add this to the pure Cu-CO contribution from cluster Ia of 1.7 eV, we still fall far short of the 3.53 eV value of cluster IIb. Thus, the component contribution cannot be estimated so simply. In the type-II clusters the Cu adlayer is stretched to be in registry with the Ru substrate. This partial breaking of the Cu-Cu bonds may artificially contribute to the enhancement of the Cu-CO bonding.

The picture of two minima, such as they appear in the type-III clusters, merging to form the unexpectedly deep wells of the type-II clusters, can be extended. If the two minima are not adjusted to perfectly superimpose, the result may be rather broad single minimum due to the "unresolved" double well. Vibrationally this would suggest large anharmonicity. By forcing the harmonic-model analysis on the system to generate the  $\omega$  values of Table II, a low value of  $\omega$  might result. We see that this appears to be the case for cluster IIa, which has the lowest  $\omega$  value (24 meV) in the Table. (However, cluster IIb does not have a particularly low value of  $\omega$  compared to the other entries in the Table.) Such low  $\omega$  values are problematic from another point of view. Given that the bulk Ru maximum phonon frequency<sup>33</sup> is  $\sim 39$  meV, significant hybridization between the substrate's modes and the single carbon-metal stretch frequency calculated herein may radically alter things.

There may be indirect experimental evidence for such mixed-metal bonding as described above. In photoemission experiments on Ru(0001) with adsorbed Cu it was noted that the Cu *d* band attenuated upon room-temperature CO dosing.<sup>1</sup> Ordinarily, at room temperature it is not expected that CO would stick to Cu. A mixed-metal bonding configuration as described above may be the explanation. Alternately, it was suggested that a chemisorption-induced segregation was drawing Ru atoms to the surface and that the Cu atoms were being covered up or were clustering.<sup>1</sup>

#### IV. SUMMARY

Total-energy and carbon-metal stretch frequency calculations were presented for a variety of small clusters configured to be analogs for the systems CO adsorbed on Cu(111), Ru(0001), and epitaxial Cu/Ru(0001). Threefold symmetric binding sites were bound to be more stable than on-top sites for the pure-metal clusters. For the mixed-metal clusters, questions were addressed concerning the modification in adsorption characteristics of the CO probe molecule relative to adsorption on a pure metal. Weakened Ru-CO binding relative to pure Ru-CO, and strengthened Cu-CO bonding relative to pure Cu was observed on the mixed metals. The importance of CO bonding simultaneously to the Ru sublayer as well as a Cu adlayer was observed. Also, on some mixed-metal clusters a subsidiary minimum was observed that could serve as a description of a precursor intermediate state to desorption.

The logical extension of the present study is to obtain carbon-metal stretch frequencies experimentally for CO adsorbed on Cu/Ru(0001). Computationally a number of problems can be examined in greater detail, as well. For instance, the effect on the total energy of making the type-II clusters incommensurate, and the evolution of the type-III clusters into type II upon continued compression of the Cu adlayer would be interesting to characterize. Twofold-symmetric bridge-bonded-site energetics, and on-top binding for the mixed-metal clusters, could also be studied. In a more general vein, the properties of epitaxial metal systems provide a fertile and challenging area for future research.

## ACKNOWLEDGMENTS

This work was supported by the National Science Foundation (under Grant No. DMR-82-14966), the U. S. Office of Naval Research (under Grant No. N00014-81-K-0438), and the U. S. Department of Energy. One of us

(S.D.B.) would like to thank the Institut für Festkörperforschung der Kernforschungsanlage, Jülich and the Physics Department and Solid State Institute of the Technion, Haifa, for their hospitality during the preparation of parts of the manuscript.

\*Permanent address: Physics Department, Zhejiang University, Hangzhou, Zhejiang, People's Republic of China.

†Permanent address: Institute of Solid State Physics, Chinese Academy of Sciences, Beijing, People's Republic of China.

<sup>1</sup>S. D. Bader, L. Richter, P.-L. Cao, D. E. Ellis, and A. J. Freeman, *J. Vac. Sci. Technol. A* **1**, 1185 (1983).

<sup>2</sup>L. Richter, S. D. Bader, and M. B. Brodsky, *J. Vac. Sci. Technol.* **18** 578 (1981).

<sup>3</sup>M. B. Brodsky and A. J. Freeman, *Phys. Rev. Lett.* **45**, 133 (1980); M. B. Brodsky, in *Novel Materials and Techniques in Condensed Matter*, edited by G. W. Crabtree and P. Vashishta (Elsevier, New York, 1982), p. 35.

<sup>4</sup>C. M. Falco and I. K. Schuller, in *Novel Materials and Techniques in Condensed Matter*, edited by G. W. Crabtree and P. Vashishta (Elsevier, New York, 1982), p. 21.

<sup>5</sup>J. H. Sinfelt, *Science* **195**, 641 (1977); *Adv. Catal.* **23**, 91 (1973); *Bimetallic Catalysts* (Wiley, New York, 1983).

<sup>6</sup>M. L. Shek, P. M. Stefan, I. Lindau, and W. E. Spicer, *Phys. Rev. B* **27**, 7277 (1983); **27**, 7301 (1983).

<sup>7</sup>J. W. A. Sachtler, M. A. Van Hove, J. P. Bibérian, and G. A. Somorjai, *Phys. Rev. Lett.* **45**, 1601 (1980); *Surf. Sci.* **110**, 19 (1981); J. W. A. Sachtler, J. P. Bibérian, and G. A. Somorjai, *ibid.* **110**, 43 (1981).

<sup>8</sup>P. J. Feibelman and D. R. Hamann, *Phys. Rev. B* **28**, 3092 (1983).

<sup>9</sup>Ding-sheng Wang, A. J. Freeman, and H. Krakauer, *Phys. Rev. B* **29**, 1665 (1984).

<sup>10</sup>K. Christmann, G. Ertl, and H. Shimizu, *J. Catal.* **61**, 397 (1980); *Thin Solid Films* **57**, 247 (1979).

<sup>11</sup>H. Shimizu, K. Christmann, and G. Ertl, *J. Catal.* **61**, 412 (1980).

<sup>12</sup>J. C. Vickerman, K. Christmann, and G. Ertl, *J. Catal.* **71**, 175 (1981).

<sup>13</sup>J. C. Vickerman, K. Christmann, G. Ertl, P. Heimann, F. J. Himpsel, and D. E. Eastman, *Surf. Sci.* **134**, 367 (1983).

<sup>14</sup>S.-K. Shi, H.-I. Lee, and J. M. White, *Surf. Sci.* **102**, 56 (1981).

<sup>15</sup>C. Q. Ma, M. V. Ramana, B. R. Cooper, and H. Krakauer, *J. Vac. Sci. Technol. A* **1**, 1095 (1983).

<sup>16</sup>J. Lee, C. P. Hanrahan, J. Arias, R. M. Martin, and H. Metiu,

*Phys. Rev. Lett.* **51**, 1803 (1983), and references therein.

<sup>17</sup>T. E. Madey and D. Menzel, *Jpn. J. Appl. Phys. Suppl.* **2**, 229 (1974); J. A. Schwarz and S. R. Kelemen, *Surf. Sci.* **87**, 510 (1979).

<sup>18</sup>J. Kessler and F. Thiene, *Surf. Sci.* **67**, 405 (1977).

<sup>19</sup>P. C. Stair, *J. Am. Chem. Soc.* **104**, 4044 (1982).

<sup>20</sup>E. J. Baerends, D. E. Ellis, and P. Ros, *Chem. Phys.* **2**, 41 (1973); V. L. Moruzzi, A. R. Williams, and J. F. Janak, *Phys. Rev. B* **15**, 2854 (1977); W. Kohn and L. J. Sham, *Phys. Rev.* **140**, A1133 (1965).

<sup>21</sup>D. E. Ellis and G. S. Painter, *Phys. Rev. B* **2**, 2887 (1970).

<sup>22</sup>A. Rosén, D. E. Ellis, H. Adachi, and F. W. Averill, *J. Chem. Phys.* **65**, 3629 (1976).

<sup>23</sup>P.-L. Cao, D. E. Ellis, and A. J. Freeman, *Phys. Rev. B* **25**, 2124 (1982); A. Rosén, E. J. Baerends, and D. E. Ellis, *Surf. Sci.* **82**, 139 (1979); D. E. Ellis, E. J. Baerends, H. Adachi, and F. W. Averill, *ibid.* **64**, 649 (1977).

<sup>24</sup>R. S. Mulliken, *J. Chem. Phys.* **23** 1833 (1955); **23** 1841 (1955).

<sup>25</sup>H. Ibach and D. L. Mills, *Electron Energy Loss Spectroscopy and Surface Vibrations* (Academic, New York, 1982), p. 1501.

<sup>26</sup>H. Ibach and D. L. Mills, *Electron Energy Loss Spectroscopy and Surface Vibrations* (Academic, New York, 1982), p. 285; T. T. Nguyen and N. Sheppard, in *Infrared and Raman Spectroscopy*, edited by R. E. Hester and R. H. J. Clark (Heyden, London, 1978), Vol. 5.

<sup>27</sup>G. E. Thomas and W. H. Weinberg, *J. Chem. Phys.* **70**, 954 (1979).

<sup>28</sup>M. A. Van Hove, R. J. Koestner, and G. A. Somorjai, *Phys. Rev. Lett.* **50**, 903 (1983).

<sup>29</sup>S. Andersson, *Surf. Sci.* **89**, 477 (1979).

<sup>30</sup>S. Andersson, *J. Vac. Sci. Technol. A* **1**, 1242 (1983); S. Andersson and N. J. Persson, *Phys. Rev. B* **24**, 3659 (1981); N. J. Persson and S. Andersson, *Surf. Sci.* **117**, 352 (1982).

<sup>31</sup>T. S. Rahman, J. E. Black, and D. L. Mills, *Phys. Rev. Lett.* **46**, 1469 (1981); *Phys. Rev. B* **25**, 883 (1982).

<sup>32</sup>J. M. Szeftel, S. Lehwald, H. Ibach, T. S. Rahman, J. E. Black, and D. L. Mills, *Phys. Rev. Lett.* **51**, 268 (1983).

<sup>33</sup>R. R. Rao and J. V. S. N. Murthy, *Z. Naturforsch.* **34a**, 724 (1979).